Available online at www.sciencedirect.com

ScienceDirect

Procedia Engineering 10 (2011) 583–588

Engineering Procedia

ICM11

Compressive Creep Behaviour of Asphalt Mixtures

Hasan Taherkhani[a*]

[a]*Civil Engineering Department, University of Zanjan, Zanjan, Iran*

Abstract

The uniaxial and triaxial steady-state deformation behaviour of a gap graded and a continuously graded asphaltic mixture have been studied. Uniaxial creep and constant strain rate tests have been conducted over a range of stress levels, strain rates and temperatures, and triaxial creep tests have been conducted over a range of deviatoric stress levels and confining pressures. The steady-state deformation behaviour of both mixtures is found to be well captured by the Modified Cross Model which predicts linear viscous behaviour at low stress levels and non-linear viscous behaviour at high stress levels. The temperature dependency of the steady-state deformation behaviour is found to be well captured by the WLF equation. It is found that confinement has a stiffening effect on the steady-state deformation behaviour which is found to be higher for the continuously graded mixture. The volumetric strain is found to increase linearly with the shear strain with a gradient that is independent of stress level and confining pressure.

Keywords: Asphalt, creep, uniaxial, triaxial, steady-state, deformation

1. Introduction

Wheel track rutting in flexible pavements can be a serious problem and permanent deformation in the asphalt layers can be a significant contributory factor. In reality, the asphaltic materials in a pavement structure is under a complex three dimensional state of stress which has a significant effect on its deformation properties. These stress conditions are difficult to replicate in laboratory, and uniaxial and triaxial testing is often undertaken.

The monotonic uniaxial and triaxial steady-state deformation behaviour of idealised bituminous mixtures (sand asphalts) was investigated by Deshpande *et al.* [1], Collop *et al.* [2] and Ossa [3]. They found that the steady-state deformation behaviour of the dense idealised mixtures (with more than 64% volume fraction of aggregate) was strongly dependent on the confining stress. For a constant stress ratio, defined as the mean stress divided by the deviator stress, the steady-state axial creep behaviour was found to have the same form as pure bitumen with linear viscous behaviour at low stress levels and non-linear viscous behaviour at higher stress levels.

The aim of this paper is to investigate the uniaxial and triaxial steady-state deformation behaviour of realistic asphaltic mixtures.

2. Materials

Two generic types of asphaltic mixture were chosen for this study; a 10mm Dense Bitumen Macadam (DBM) [4] and a 30/10 Hot Rolled Asphalt (HRA) [5]. Granite aggregates and a 70/100 penetration grade of bitumen were used to produce both mixtures. The target air voids content was chosen to be 4% for both mixtures and binder contents of 5.5% and 8% were chosen for the DBM and HRA respectively.

* Corresponding author. Tel.:00982813691681;fax:00982415152611
E-mail address: Taherkhani.hasan@yahoo.com.

 doi:10.1016/j.proeng.2011.04.097

Cylindrical specimens, 100mm in diameter and 100mm in height, were manufactured for the testing programme. The specimens were stored in a cold room at 5˚C until they were required for testing.

3. Test Equipment and Instrumentation

An Instron 1332 loading frame with a temperature-controlled cabinet (–5˚C to 50˚C) and a servo-hydraulic actuator with a load capacity of ±100 kN and ±50mm axial stroke was used for the testing programme. For uniaxial tests, the specimen is placed between two polished chrome plates. A friction reduction system was used to minimize lateral confinement due to friction between the platens and the specimen. Two LVDTs, positioned on the top platen were used to measure the axial deformation of the specimen.

The triaxial testing equipment comprised three main parts, the servo-control hydraulic machine as described above, a triaxial cell placed in the temperature-controlled cabinet, and an air compressor to apply the confining pressure. An impervious latex membrane was used to seal the specimens from the air inside the cell, which was used as the confining medium. The axial deformation of the specimen was measured using the load line displacement of the actuator.

4 Test Procedure

4.1 Uniaxial Tests

Uniaxial constant strain rate and constant stress creep tests were performed over a range of strain rate and stress levels, and temperatures (10^{o}C to 40^{o}C). To ensure uniformity of temperature, the specimens were stored in the temperature-controlled cabinet for at least 12 hours prior to testing. The specimen was instrumented and a small compressive pre-load was applied to take up any slack in the system and allow the friction reduction system to deform in order to minimise subsequent measurement errors. A constant load or displacement rate was then applied to the specimen until failure. Axial deformations and load measurements at pre-set time intervals were logged automatically during the test.

4.2 Triaxial Tests

The target confining pressure was applied to the specimen followed by the preloading stress which was immediately followed by the target axial stress. The axial and radial deformations were automatically logged by the computer connected to the equipment for the duration of the test.

In the triaxial tests, because of axial symmetry, two of the principle stresses are equal to the confining stress. The third principal stress is equal to the sum of the confining stress and an additional axial stress which is applied.

The mean stress Σ_m is the average of three principle stresses, and the deviator stress (Σ) acting on the specimen are given by:

$$\Sigma_m = \frac{\Sigma_{33} + \Sigma_{11} + \Sigma_{22}}{3} = p + \frac{Q}{3A} \tag{1}$$

$$\Sigma = \Sigma_{33} - \Sigma_{11} = \frac{Q}{A} \tag{2}$$

Triaxial tests were performed at 35°C over the range of stress ratio, $\eta = \Sigma_m / \Sigma$, and deviator stress levels (Table 1). The HRA was tested up to a maximum stress ratio of η=0.7, whereas the DBM was only tested up to a maximum stress ratio of 0.56. This was because stress ratios above these values resulted in specimen lock-up and gave no meaningful results.

Table1: Triaxial test conditions

Mixture	Stress Ratio	Deviator Stress (kPa)
HRA30/10	0.33, 0.563, 0.7	300, 500, 700
10mm DBM	0.33, 0.463, 0.563	500, 750, 1000

5. Test Results

5.1 Uniaxial Test Results

Typical uniaxial creep test results for the 10 mm DBM at selected testing conditions are presented in Figure 1, where the axial strain is plotted against time. It can be seen from this figure that the creep curve can be divided into three regions: a primary creep region where the strain rate decreases, a secondary creep region where the strain rate is almost constant, known as the steady-state strain rate, and a tertiary creep region where the strain rate increases rapidly.

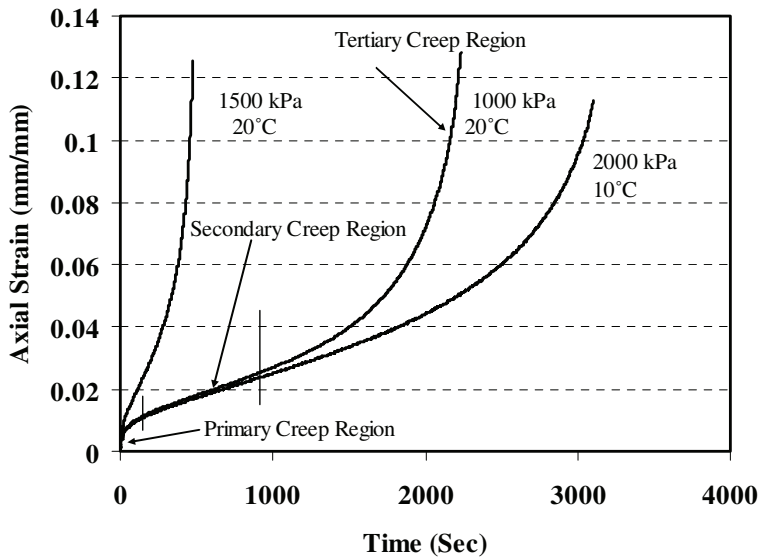

Fig. 1 Typical uniaxial creep test results for the 10 mm DBM.

Figure 2 shows typical results from constant strain rate tests on the 10 mm DBM at a selected test conditions, where axial stress is plotted against the axial strain. It can be seen from this figure that there is an increase in the steady-state stress with increasing strain rate and/or decreasing temperature. It was found that the steady-state stress values for the DBM were greater than those for the HRA30/10.

The steady-state results from the constant stress creep and constant strain rate tests for the HRA are summarised in Figure 3, where the steady-state strain rate is plotted against the steady-state stress on double logarithmic scales. Similar behaviour was observed for the DBM which, for brevity, is not presented here. The steady-state stress in the constant strain rate tests is the peak stress at the prescribed strain rate and the steady-state strain rate in constant stress creep tests is the slope of the secondary creep region. It has previously been found that results from creep tests and constant strain rate tests are complementary [6, 3, 7 and2].

Cheung [6] and Deshpande [8] proposed the Modified Cross Model to relate the steady-state stress to the steady-state strain rate:

$$\sigma = \frac{\sigma_0 \dot{\varepsilon}}{\dot{\varepsilon}_p} \left\{ 1 + \left(\frac{\dot{\varepsilon}}{\dot{\varepsilon}_p} \right)^m \right\}^{-1} \qquad (3)$$

where σ is the uniaxial stress, $\dot{\varepsilon}$ is the uniaxial strain-rate and $\sigma_0, m, \dot{\varepsilon}_p$ are material constants.

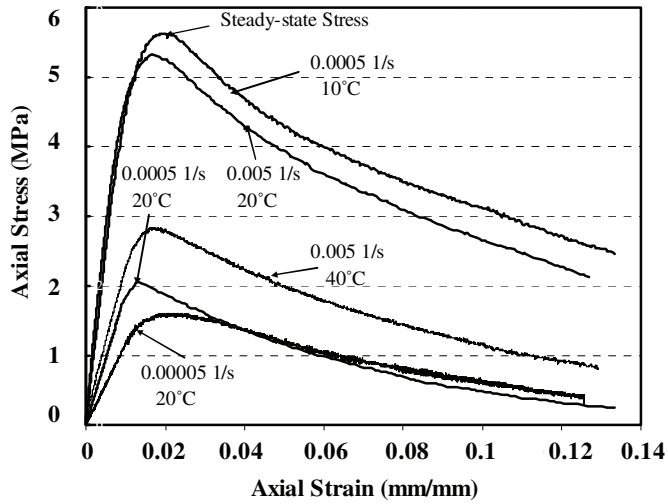

Fig.2 Typical constant strain rate test results for the 10 mm DBM.

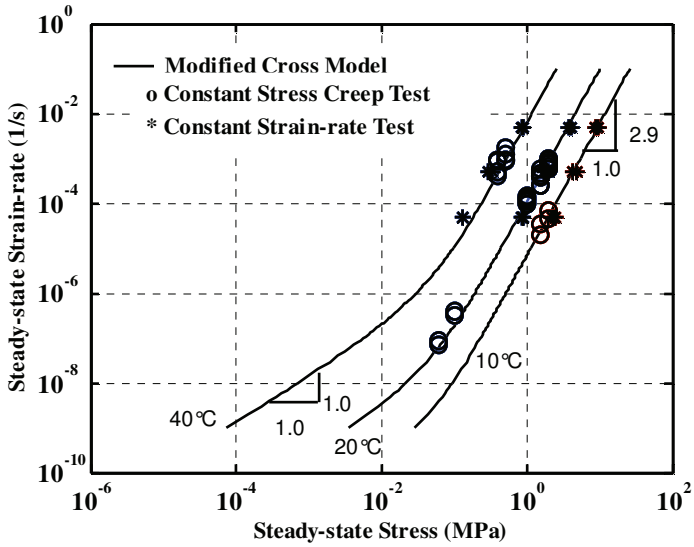

Fig. 3 Uniaxial steady-state deformation behaviour for the HRA30/10.

It can be seen that for low values of $\dot{\varepsilon}$ Equation (4) reduces to linear viscous behaviour ($\dot{\varepsilon} \propto \sigma$) and for high values of $\dot{\varepsilon}$ Equation (3) reduces to non-linear viscous behaviour ($\dot{\varepsilon} \propto \sigma^n$) where the exponent *n* is given by $1/(1-m)$. The solid lines in Figure 5 are predictions from the modified Cross model.

For the three temperatures investigated in this study, the temperature dependency of the HRA and DBM mixtures was found to be well captured by the free volume WLF model, which can be incorporated into Equation (4) through the constant $\dot{\varepsilon}_p$ [6] giving:

$$\dot{\varepsilon}_p = \dot{\varepsilon}_{pc} \exp\left(\frac{2.303 c_1^s (T - T_s)}{c_2^s + (T - T_s)} \right) \quad (4)$$

where $\dot{\varepsilon}_{pc}$ is the reference strain rate at T=0°C, c_1^s & c_2^s = universal constants with the values 8.86 & 101.6 and T_s is the reference temperature with the value of 30°C. Equations (3) and (4) were fitted to the data; the constants are given in Table 2.

Table 2: Modified Cross Model constants for the mixtures.

Parameter	HRA	DBM
σ_0 (MPa)	0.041	0.1
$\dot{\varepsilon}_{pc}$ (1/s)	8.7×10^{-8}	8.7×10^{-9}
m	0.66	0.75

5.2 Triaxial Tests Results

Figure 4 summarises the monotonic triaxial steady-state behaviour of the HRA over a range of deviator stresses σ and stress ratios η, where the steady-state strain rate $\dot{\varepsilon}$ is plotted against stress σ on double logarithmic scales. Similar behaviour was observed for the DBM, which for brevity, is not presented here. It can be seen from Figure 4 that, for a constant stress ratio, the curves have the same shape as the curve for uniaxial behaviour (η=1/3) shown in Figure 5.

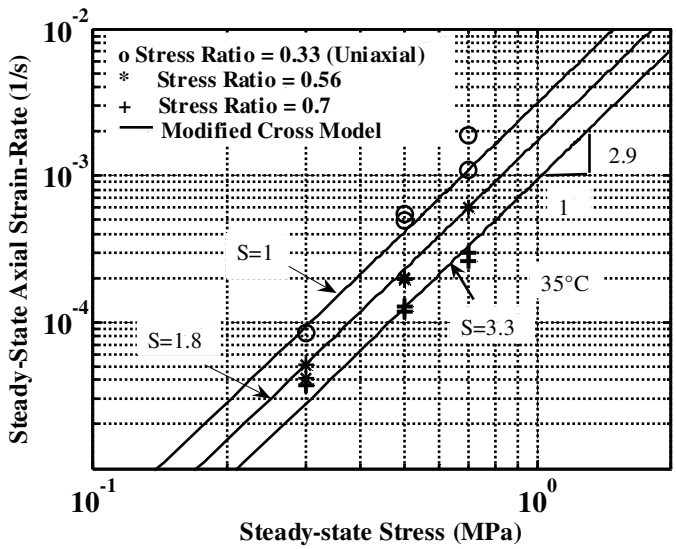

Fig. 4 Monotonic steady-state behaviour of the HRA at different stress ratios.

The Modified Cross Model with the addition of a stiffening factor (as suggested by Deshpande *et al.* [1] is given by:

$$\frac{\sigma}{\sigma_0} = \frac{\dot{\varepsilon}}{S\dot{\varepsilon}_p} \left\{ 1 + \left(\frac{\dot{\varepsilon}}{S\dot{\varepsilon}_p} \right)^m \right\}^{-1} \quad (5)$$

where S is the stiffening factor. The value of S was determined by fitting Equation (5) to the experimental data using the constants in Table 2. The result is shown in Figure 4 by the solid lines. It can be seen from Figure 4 that, over the range of stress levels used in this study, the mixtures exhibits non-linear power law creep behaviour with the power exponent of 2.9. From Figure 5 it can be seen that S increases with increasing the stress ratio η. Figure 5 summarises the effect of the stress ratio on S for the two mixtures. It can be seen from this figure that the stiffening factor is more sensitive to stress ratio for the DBM compared to the HRA mixture. This was expected as the confinement has more effect where there is greater aggregate interlock which is the case for the continuously graded DBM.

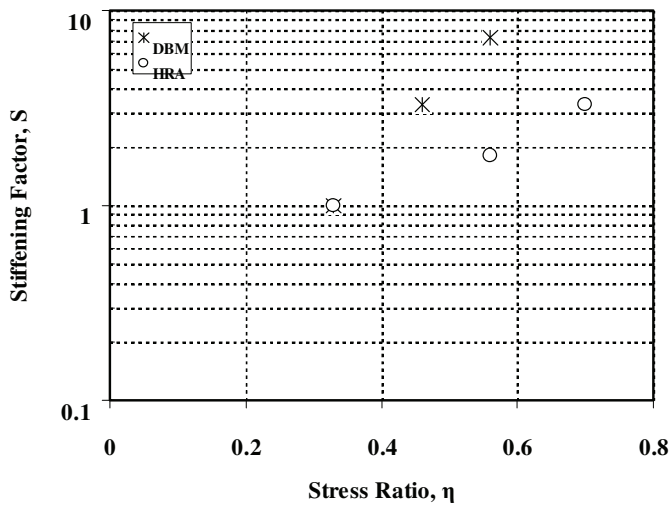

Fig. 5 Stiffening factor of the mixtures.

6. Conclusions

The following conclusions can be drawn from this paper:

- The uniaxial and triaxial steady-state deformation behaviour of the HRA and the DBM mixtures was found to be linear viscous at low stress levels and non-linear viscous with an exponent of 2.9 for the HRA and 4 for the DBM mixture at high stress levels. The behaviour was found to be well captured by the modified Cross model.
- The temperature dependency of the uniaxial steady-state deformation behaviour was found to be well captured by WLF equation.
- Confinement was found to have a stiffening effect on the steady-state deformation behaviour with a greater effect for the mixture with the higher aggregate interlock.
- A critical stress ratio was found for each mixture, beyond which the mixtures were observed to lock-up.

References

[1] Deshpande, V. and Cebon, D. Steady-state constitutive relationship for idealised asphalt mixes. *Journal of Mechanics of Materials* 31 (4): 271-297, 1999.

[2] Collop, A. C. and Khanzada, S. Permanent deformation in idealised "Sand Asphalt" bituminous mixtures. *The International Journal of road Materials and Pavement Design* 2(1): 7-28, 2001.

[3]Ossa, E.A. Deformation behaviour of bitumen and bituminous mixes. Ph.D. thesis,

[4]British Standards Institution. Sampling and examination of bituminous mixtures for roads and other paved areas. *Methods of test for the determination of density and compaction*, 1989.

[5] British Standards Institution. Hot rolled asphalt for roads and other paved areas. BS 594:Part1, London, 2003.

[6] Cheung, C. Y. Mechanical behaviour of bitumens and bituminous mixes. *Ph.D. Thesis,* University of Cambridge, Cambridge, 1995.

[7] Collop, A. C. and Khanzada, S. Permanent deformation behaviour of idealised bituminous mixtures. *Proc. 3rd European symposium on performance and durability of bituminous materials and hydraulic stabilised composites*, Leeds UK, 47-58, 1999.

[8] Deshpande, V.S. Steady-state deformation behaviour of bituminous mixes. *Ph.D. Thesis*, University of Cambridge, UK, 1997.